

Correlated UV Through IR Signature Modeling of Targets and Backgrounds

November 1998

John M. Stewart, Robert W. Goodwin,
Melinda K. Higgins, and Ed M. Patterson

GTRI, Georgia Institute of Technology

Atlanta, GA 30332

Abstract

Simulations of the performance of multi-spectral sensors or multiple sensors with data fusion require phenomenological consistency in the target and background signatures presented to the sensors. This paper describes the incorporation of ultraviolet signatures of targets and backgrounds into an engagement simulation framework. This paper emphasizes ultraviolet phenomenology and the signatures of aircraft compared to fires, lights, industrial sources and other high energy sources. In particular, variation of the sources as a function of time, wavelength and aspect angle is discussed, as these variations may be critical to the discrimination of targets from natural and man-made background sources. The organization of multiple data sets representing the same object in different spectral regions is also described for use in simulations.

REPORT DOCUMENTATION PAGE

Form Approved OMB No.
0704-0188

Public reporting burden for this collection of information is estimated to average 1 hour per response, including the time for reviewing instructions, searching existing data sources, gathering and maintaining the data needed, and completing and reviewing this collection of information. Send comments regarding this burden estimate or any other aspect of this collection of information, including suggestions for reducing this burden to Department of Defense, Washington Headquarters Services, Directorate for Information Operations and Reports (0704-0188), 1215 Jefferson Davis Highway, Suite 1204, Arlington, VA 22202-4302. Respondents should be aware that notwithstanding any other provision of law, no person shall be subject to any penalty for failing to comply with a collection of information if it does not display a currently valid OMB control number. PLEASE DO NOT RETURN YOUR FORM TO THE ABOVE ADDRESS.

1. REPORT DATE (DD-MM-YYYY) 01-11-1998	2. REPORT TYPE Conference Proceedings	3. DATES COVERED (FROM - TO) xx-xx-1998 to xx-xx-1998
---	--	--

4. TITLE AND SUBTITLE Correlated UV Through IR Signature Modeling of Targets and Backgrounds Unclassified	5a. CONTRACT NUMBER
	5b. GRANT NUMBER
	5c. PROGRAM ELEMENT NUMBER

6. AUTHOR(S) Stewart, John M. ; Goodwin, Robert W. ; Higgins, Melinda K. ; Patterson, Ed M. ;	5d. PROJECT NUMBER
	5e. TASK NUMBER
	5f. WORK UNIT NUMBER

7. PERFORMING ORGANIZATION NAME AND ADDRESS GTRI Georgia Institute of Technology Atlanta, GA30332	8. PERFORMING ORGANIZATION REPORT NUMBER
--	--

9. SPONSORING/MONITORING AGENCY NAME AND ADDRESS Director, CECOM RDEC Night Vision and Electronic Sensors Directorate 10221 Burbeck Road Ft. Belvoir, VA22060-5806	10. SPONSOR/MONITOR'S ACRONYM(S)
	11. SPONSOR/MONITOR'S REPORT NUMBER(S)

12. DISTRIBUTION/AVAILABILITY STATEMENT
APUBLIC RELEASE

13. SUPPLEMENTARY NOTES
See Also ADM201041, 1998 IRIS Proceedings on CD-ROM.

14. ABSTRACT
Simulations of the performance of multi-spectral sensors or multiple sensors with data fusion require phenomenological consistency in the target and background signatures presented to the sensors. This paper describes the incorporation of ultraviolet signatures of targets and backgrounds into an engagement simulation framework. This paper emphasizes ultraviolet phenomenology and the signatures of aircraft compared to fires, lights, industrial sources and other high energy sources. In particular, variation of the sources as a function of time, wavelength and aspect angle is discussed, as these variations may be critical to the discrimination of targets from natural and man-made background sources. The organization of multiple data sets representing the same object in different spectral regions is also described for use in simulations.

15. SUBJECT TERMS

16. SECURITY CLASSIFICATION OF:	17. LIMITATION OF ABSTRACT Public Release	18. NUMBER OF PAGES 10	19. NAME OF RESPONSIBLE PERSON Fenster, Lynn lfenster@dtic.mil
---------------------------------	--	---------------------------	--

a. REPORT Unclassified	b. ABSTRACT Unclassified	c. THIS PAGE Unclassified	19b. TELEPHONE NUMBER International Area Code Area Code Telephone Number 703767-9007 DSN 427-9007
---------------------------	-----------------------------	------------------------------	--

1 Introduction

Traditionally GTSIMS missile flyout simulations have consisted of a missile, a target and a background. Backgrounds were composed primarily of natural features such as sky, water, rocks, roads, fields and trees. These features are generally adequate since most infrared missiles have small field of views, short flight times and upward launch geometries, making the possibility of other man made objects in the background low.

Under the ATIRCM/CMWS program we have been refining the capability to test optical missile warning receivers (MWRs) as players in closed loop simulations. Optical missile warning receivers employ sensors with a up to a 4π sr field of regard, and these devices scan this field of regard for sources that match the characteristics of threat missiles. The large fields of regard of these systems along with their need to watch the ground for long periods of time translate to a high probability that man-made objects other than the threat will be visible to the MWR during a simulation.

Threat missiles typically have energetic plumes that are brighter than most natural background objects. However, a number of common objects such as lights, fires, aircraft plumes, welders, pyrotechnic flares, bombs and other weapons can be least as energetic as missile plumes. As part of the background, these sources can have two major effects on the systems being tested. First, they can cause false positives which reduce pilot confidence in the system. Second, as clutter objects, they can conceal the true threat.

In order to properly test systems in the presence of these sources, a database of sources was constructed from measured data and predictive codes. Framework was added to the simulation so that many of these sources can be easily added to the simulation.

This paper discusses flexibility provided by the model framework, lists the background and target sources available in the simulation and discusses efforts to model specific sources in the ultra-violet (UV) region of the spectrum.

2 Object Descriptions

Any object in the simulation that emits or interacts with radiation from UV through IR wavelengths is summarized by a visible object file which tells the simulation how to present the object to a different sensors that are in the simulation. The different classes of sensors are mainly defined by their wavelength character-

istics such as UV, near IR, mid IR etc. The classes also separate sensors that are likely to resolve the target with many pixels and process the resulting spatial pattern from sensors that are never likely to resolve the target. Examples of resolved and unresolved sources in the simulation are shown in figure 1.

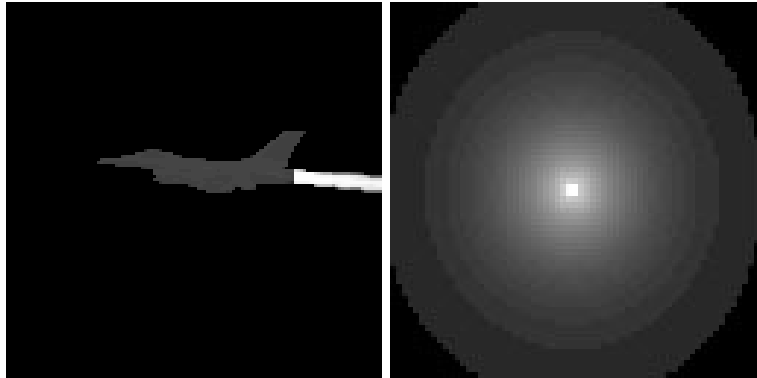


Figure 1: An F-16 in full afterburner shown as a resolved infrared source and an unresolved UV source. Range to target is approximately 1Km. IR field of view is 1.5 degrees and UV field of view is 100 degrees. LOWTRAN 7 was used for IR atmospheric effects and OSIC 7.0 was used for UV effects. Images have been processed to show relevant features.

Resolved objects require inputs to the visible and infrared scene renderer, GTVISIT. These inputs include faceted target geometry files, surface temperatures, surface optical properties, plume flowfields, and matching atmospheric parameters. The GTVISIT software is described in [1].

For unresolved objects one of the most important cues is the signature variation verses time. To a sensor, an object's temporal variation depends on its inherent temporal signature, its change in location with respect to the sensor, its change in orientation, and changes in spectral output that change the atmospheric transmittance from the source to the sensor. For short wavelengths, the scatter pattern that reaches the sensor can also be an important detail and it is dependent on the object's spatial distribution as well as atmospheric properties.

In order to represent each of these aspects, the radiant intensity of the point object, J is dependent on two aspect angles, θ and ϕ , time, t , altitude, a , and velocity v . In the simulation the radiant intensity of a source can be expressed as the product of multipliers shown below

$$J(\lambda, \theta, \phi, t, \delta t, a, v) = S_f(\lambda, \delta\lambda)J(t)A(\theta, \phi)P(a)V(v) \quad (1)$$

where $A(\theta, \phi)$ is an aspect angle function that defines the relative magnitude of the source viewed from different angles. $P(a)$ is a multiplier dependent on altitude and $V(v)$ is a multiplier dependent on velocity. The spectral multiplier, $S_f(\lambda, \delta\lambda)$ defines the portion of $J(t)$ that is distributed between λ and $\lambda + \delta\lambda$.

$$S_f(\lambda, \delta\lambda) = \frac{\int_{\lambda}^{\lambda+\delta\lambda} S(\lambda)d\lambda}{\int_{\lambda_{min}}^{\lambda_{max}} S(\lambda)d\lambda} \quad (2)$$

where $S(\lambda)$ is a spectral distribution function and λ_{min} and λ_{max} are the minimum and maximum wavelengths in the point signature definition.

In the cases where the signature can be defined as a sum of products, the functions in equation 1 are input as a series of ASCII tables. The ASCII tables are generally small and loop constructs are provided to play back periodic sources. When there is coupling between the functions, an entire table of $J(\lambda, \theta, \phi, t, \delta t, a, v)$ values can be entered directly as a binary table which is encoded for portability across machines.

Class	Specific Examples
Flares	M206, MJU7A/B, MJU10, MJU8B, MK46, MJU47, MJU48, XM212, LUU2B
Fires	Diesel, gasoline, wood, JP-8
Lights	High intensity discharge and quartz tungsten halogen
Welders	Stick welders, gas tungsten arc welders
Aircraft	F-16 Pratt and Whitney F100 and GE 110 Engines, F15
Munitions	m57c02, m57c08, m57c10, m831a1, m865e3, m934 mk82 mk83 mk84

Table 1: List of point sources available to the simulation.

Sources that are included in the simulation are listed in table 1. The munitions signatures are contributed by SciTec and are visible only in the UV portion of the simulation.

3 Trajectories and Simulation Geometry

Another cue for the discrimination of unresolved sources is motion. Objects can be eliminated from consideration if predictions of their velocities are too high or too low. Other motion cues can be obtained from predictions of object direction relative to the sensor.

In the simulation object, trajectories originate from one of two places. Missiles, some aircraft, and counter measure flare trajectories are products of the closed loop simulations. In these cases, an initialization phase communicates information in the visible object file to executables that need it to generate imagery for a particular sensor. Once the initialization is complete, position and orientation updates are sent as they are required. Other background objects also also associated with motion. Examples are rotating navigation beacons, illumination flares like the LUU2B, and sources on missiles or other aircraft not involved in the closed loop portion of the simulation. For these sources a simulation object was added to read a list of point sources and broadcast the initialization and kinematic update messages for each source. The point source manager uses a cubic spline fit to trajectory data for position and orientation updates.

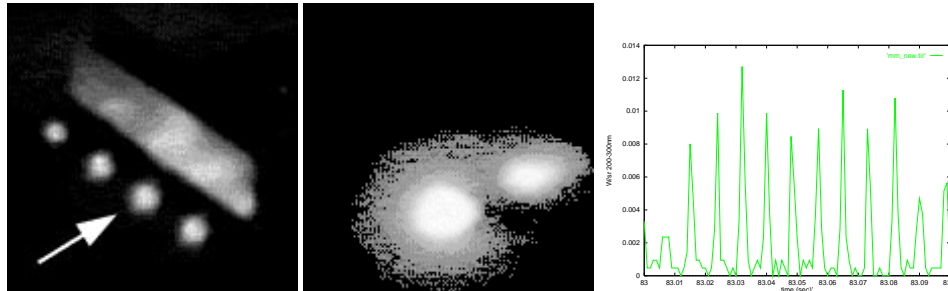


Figure 2: Billboard with Metal Halide Lamp in the visible, UV and UV temporal trace. One damaged lamp and its reflection is visible in the UV image collected by the MWIP program [3].

As mentioned above, change in relative positions of the sensor and object changes the apparent temporal trace seen by the sensor. This modulation primarily results from range squared fall off and change in atmospheric transmission with range. Another source of trajectory related modulation is local obscuration of the source. Figure 2 demonstrates a common example of this phenomena. A damaged

metal halide lamp illuminates a billboard. From one side of the billboard, the lamp and its reflection are clearly visible, but neither are visible from the opposite side.

The GTVISIT software keeps track of some obstructions between sensors and the target, but this technique is not generally applicable for missile warning receiver applications because the large area visible in the warning receiver field of view and a small facet size needed to reduce surface error near the source require too many facets for practical rendering times. For geometries involving walls or rectangular enclosures, a utility is provided to compute obstruction and diffuse reflection. The output of the utility is an aspect angle dependence function which can be added to the point signature file. Figure 3 demonstrates a fly over of the billboard from the back of a simulated billboard illuminated by a single lamp. When the sensor approaches from the back, it never directly sees the lamp or the reflection. As a result, the recorded signal decreases as the sensor approaches because the billboard blocks a larger portion of the scattered light from the source.

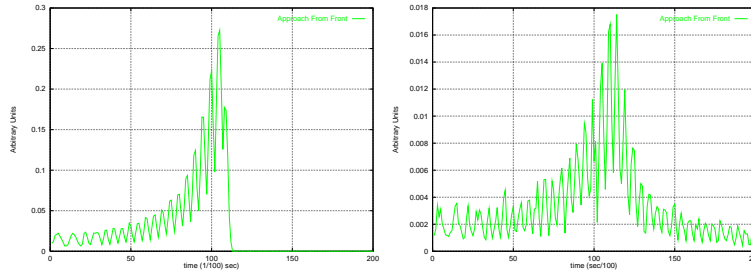


Figure 3: Sensor output when approaching the billboard from the front and the back. The sensor is pointed forward and passes 40 meters above the source. Initial range is 500 meters.

The temporal characteristics of the lamp used in this example come from examination of Metal Halide and Mercury Vapor lamps measured under MWIPS and by the CMWS program. Based on these measurements, a fit for the radiant intensity of the lamp is defined

$$J(t) = J_o \left| \sin \left(2\pi \omega_d \frac{t}{N} \right) \right| * \delta \left(t - \frac{j}{2.0\omega} \right) \quad (3)$$

Where J_o is the peak intensity of the lamp output, N is the sample rate in samples/sec. $\omega_d = \omega/D$ where ω is the power line frequency in Hz and D

is a duty cycle factor. $\delta()$ is the Dirac delta function, and $i \leq N/2$. The temporal distance between lamp pulses is $1/2\omega$ and the width of the pulses at zero amplitude is $1/2\omega_d$. In some cases, the resulting time sequence is filtered with a single time constant filter [3]. The peak radiant intensity is a function of lamp wattage and construction. Magnitudes for intensity and spectral output are taken from measurements and references on UV light output such as [4].

Since the lamps are small, they are also treated as point sources in the infrared. The primary source of output from the IR lamps was assumed to be emission from the glass bulbs, heated fixtures and filaments of quartz lamps. Steady state thermal analysis was performed to predict average temperatures of lamps. In the case of the 400 Watt metal halide lamp on the billboard, about half of the energy used by the lamp is dissipated by heat [5]. The spectral distribution functions used by the model are shown in figure 4.

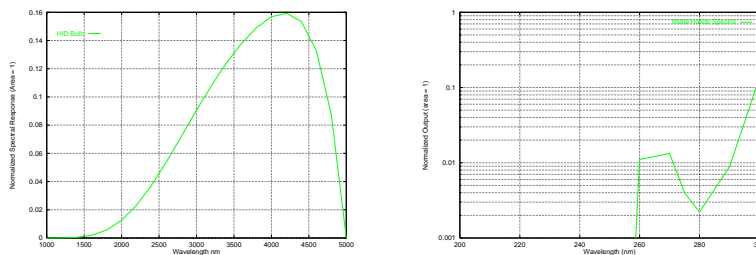


Figure 4: UV and IR normalized spectral output of Metal Halide lamp and enclosure. The IR spectra is a gray body spectra computed from bulb and lamp temperature. The UV spectra is from a Sylvania MetalarcTM digitized from Sliney [4]

4 Aircraft Signatures

For aircraft mounted UV sensors, afterburners are of special interest for two reasons. First, they can generate a large quantity of UV radiation which can interfere with the operation on board sensors. Second, as fast moving combustion sources, they can cause false positives.

Modeling in this area started with extensive ground measurements of F-16 and F-15 aircraft at Eglin AFB [7] [6]. These measurements included corre-

lated IR and UV measurements but only consider the aircraft operating tied to the ground at sea level. Additional fixed wing measurements at 10Kft were made of afterburners and countermeasure flares using a CMWS prototype [8]. While these measurements were not well calibrated, they include TSPI and provide some useful bounds on UV signatures.

Because the data sets used for the PFAS afterburner models are limited, it is useful to compare the output of radiative plume models like SPF-III[9] / SPURC[10]. If the model predictions agree with the measured signatures, they can be used to provide guidance for the scaling of plume signatures to the operational velocities and altitudes not measured during the ground test. The comparison is also useful because the infrared signatures in the simulation were already dependent on radiative plume models. If the model could use the same inputs to accurately predict the plume signature in both regions, confidence in the model would be increased.

Since SPF-III and SPURC had not been utilized to model aircraft afterburner plumes at the wavelengths of interest, the capabilities and limitations of the models were evaluated to provide information on the sensitivity of the models to changes in parameters and inputs.

Our approach was to compare the predicted spectra and plume size using the same inputs for both the infrared and UV portions of the spectrum to the ground data collected at Eglin. The details of the code analysis are beyond the scope of this paper, but there was good agreement of model predictions to measured infrared and UV plume lengths and overall radiant intensities. This agreement required some changes to the turbulence model in SPF-III and some changes to the plume chemistry model in SPURC [11]. The infrared spectra also agreed well, but the UV spectra did not as the model predicts a color temperature that was significantly lower than the data suggest.

The primary source of UV photons in afterburning plumes is chemiluminescent emission from $\text{CO} + \text{O}$ resulting from the oxidation of soot in the plume. The code was traced to fundamental $\text{CO} + \text{O}$ emission properties reported in [12] and the code was found to be making predictions consistent with this data.

Based on the good match to UV radiant intensity and plume size, the UV output from the model was used to formulate a table for altitude and velocity scaling functions $P(a)$ and $V(v)$. The spectral distribution and aspect angle factors were retained from measured data. Afterburner signatures with steady state and start up transients are included in the database.

5 Conclusion

This paper outlines the development of a UV signature database of emitters that match IR emitters in a closed loop simulation.

References

- [1] Hetzler, Morris C. and J Stewart "Enhancements to GTVISIT and Its Use of Sensor Models for the Multi-Spectral Threat VISEO Program" *1997 Meeting of The IRIS Specialty Group on Camouflage, Concealment and Deception Volume I* p233.
- [2] Crow, Katherine M. and T Nau. *OSIC version 7.0 Model Description and User's Manual* SciTec, Inc. Princeton, NJ. May 1998.
- [3] Glover, R. E., E. M. Patterson, L. Little, W. G. Robinson, J. H. Hallman "Results of the Missile Warning Improvement Program AAR-47 Missile Warning System False Alarm Data Collection" *1998 Meeting of The IRIS Specialty Group on Countermeasures* April 8, 1998.
- [4] Sliney and Wolbarsht, "Safety with Lasers and Other Optical Sources", Plenum Press, 1980.
- [5] On-line lighting handbook at University of Kansas, <http://www.arce.ukans.edu/book>.
- [6] Baker, K. P.; Lowry III, H. S.; Reed, R. A.; Roberds, D. W.; Simmons, M. A.; Ready, J. A.; Lewis, G. W.; *AEDC-TR-97-2: Common Missile Warning System (CMWS) Potential False Alarm Source (PFAS) Tests 1A and 1B*, K. L. Dietz, editor; Sverdrup Technology, Inc. AEDC Group, Arnold AFB, TN, February 1997.
- [7] Memo from Mark T. Allen at SciTec. Eglin I Data Analysis, December 5, 1996.
- [8] "Eglin II" - Fixed Wing PFAS" Data originally provided by Sanders a Lockheed Martin Corp and distributed by Macaulay Brown, Inc.

- [9] Pergament, H.S.; Taylor, M. W. *Standardized Plume Flowfield Module (SPF-III) Version 4.0: Volume I Model Formulation and Numerical Algorithms and Volume II Program User's Manual*, Propulsion Science and Technology, Inc., Princeton, NJ, February 1998. [Prepared for: Ballistic Missile Defense Organization, Air Force Research Laboratory/PRSA, Army Aviation and Missile Command, Arnold Engineering Development Center and National Air Intelligence Center by Propulsion Science Technology, Inc., 91 Wall Street, Research Park, Princeton, NJ, 08540, (609)924-1070]
- [10] *Standard Plume Ultraviolet Radiation Code (SPURC), Version LA1.3: User's Manual*, Air Force Phillips Laboratory, Edwards AFB, CA, March 1997. [Air Force Phillips Laboratory, OL-AC PL / RKFT, Edwards AFB, CA 93524-7230, Air Force Contract F04611-87-C-0087]
- [11] Hal Pergament at Propulsion Science Technology suggested the changes.
- [12] Slack, M; Grillo, A. "High Temperature Rate Coefficient Measurements of CO + O Chemiluminescence," *Combustion and Flame*, **1985**, 59, 189-196.